

Supporting Information for

Controlled Doping of Semiconducting Titania Nanosheets for Tailored Spinelectronic Materials

Minoru Osada,^{a,b,*} Satoshi Yoguchi,^a Masayuki Itose,^a Bao-Wen Li,^a Yasuo Ebina,^{a,b}
Katsutoshi Fukuda,^c Yoshinori Kotani,^d Kanta Ono,^d Shigenori Ueda^e and Takayoshi Sasaki^{a,b}

^a International Center for Materials Nanoarchitectonics (MANA), National Institute for Materials Science (NIMS), Tsukuba, Ibaraki 305-0044, Japan

^b CREST, Japan Science and Technology Agency, Kawaguchi, Saitama 332-0012, Japan

^c Research & Development Initiative for Scientific Innovation of New Generation Batteries (RISING), Kyoto University, Hyogo 679-5198, Japan

^d Institute of Materials Structure Science, High Energy Accelerator Research Organization (KEK), Tsukuba, Ibaraki 305-0801, Japan

^e NIMS Beamline Station at SPring-8, National Institute for Materials Science (NIMS), Hyogo 679-5148, Japan

*E-mail. osada.minoru@nims.go.jp

Table 1. Refined lattice parameters of Fe,Co-doped layered titanates and their exfoliated nanosheets.

Table 2. Chemical analysis results of Fe,Co-doped layered titanates and acid-exchanged forms.

Figure S1. XRD patterns of Fe,Co-doped layered titanates.

Figure S2. XRD patterns of acid-exchanged forms.

Figure S3. Variation of the in-plane lattice parameters of protonic titanates and exfoliated nanosheets.

Figure S4. Raman spectra of (Fe/Co)-codoped layered titanates.

Figure S5. UV-Visible absorption spectra for multilayer films of [PDDA/Ti_{1-x-y}Fe_xCo_yO₂]_n.

Figure S6. First-principles DFT calculations on the magnetic properties of Ti_{1-x}Fe_xO₂, Ti_{1-y}Co_yO₂ and Ti_{1-x-y}Fe_xCo_yO₂ nanosheets with different oxidation states.

Figure S7. Resistivity versus the reciprocal temperature of Ti_{0.75}Fe_{0.1}Co_{0.15}O₂ nanosheets.

Table 1. Refined lattice parameters of Fe,Co-doped layered titanates and their exfoliated nanosheets.

		<i>a</i> (nm)	<i>b</i> (nm)	<i>c</i> (nm)
Fe-doping [K _{0.8} Ti _{(5.2-2x)/3} Li _{(0.8-x)/3} Fe _x O ₄]				
<i>x</i> = 0	as-prepared	0.38266(1)	1.5510(1)	0.29730(1)
	acid-exchanged	0.37809(1)	1.8240(1)	0.30024(1)
	nanosheet	0.37675(1)		0.29715(6)
<i>x</i> = 0.2	as-prepared	0.38208(1)	1.5566(1)	0.29719(1)
	acid-exchanged	0.37821(1)	1.8103(1)	0.30011(1)
	nanosheet	0.37676(8)		0.29797(6)
<i>x</i> = 0.4	as-prepared	0.38225(1)	1.5569(0)	0.29756(1)
	acid-exchanged	0.38225(1)	1.5569(0)	0.29756(1)
	nanosheet	0.37645(7)		0.29871(0)
<i>x</i> = 0.6	as-prepared	0.38202(1)	1.5600(0)	0.29756(1)
	acid-exchanged	0.37692(1)	1.8192(1)	0.30086(1)
	nanosheet	0.37672(8)		0.29948(4)
<i>x</i> = 0.8	as-prepared	0.38137(1)	1.5676(1)	0.29740(1)
	acid-exchanged	0.37615(1)	1.8177(1)	0.30157(1)
	nanosheet	0.37733(9)		0.30048(5)
Co-doping [K _{0.8} Ti _{(5.2-y)/3} Li _{(0.8-2y)/3} Co _y O ₄]				
<i>y</i> = 0.1	as-prepared	0.38293(2)	1.5517(1)	0.29776(2)
	acid-exchanged	0.37924(1)	1.7932(0)	0.29911(1)
	nanosheet	0.37646(8)		0.29766(4)
<i>y</i> = 0.2	as-prepared	0.38265(1)	1.5560(1)	0.29777(2)
	acid-exchanged	0.37891(2)	1.7808(0)	0.29927(1)
	nanosheet	0.37656(1)		0.298471(5)
<i>y</i> = 0.3	as-prepared	0.38271(1)	1.5578(1)	0.29786(2)
	acid-exchanged	0.37829(2)	1.7824(0)	0.29987(1)
	nanosheet	0.3771(1)		0.29948(7)
<i>y</i> = 0.4	as-prepared	0.38263(1)	1.5599(1)	0.29787(1)
	acid-exchanged	0.37792(2)	1.7855(1)	0.30082(2)
	nanosheet	0.3775(1)		0.30039(9)

(Continued)

		<i>a</i> (nm)	<i>b</i> (nm)	<i>c</i> (nm)
Fe/Co-codoping [K _{0.8} Ti _{1.6-x/2} Fe _x Co _{0.4-x/2} O ₄]				
<i>x</i> = 0.2	as-prepared	0.38223(2)	1.5614(1)	0.29776(1)
	acid-exchanged	0.37776(2)	1.7904(1)	0.30079(2)
	nanosheet	0.3774(1)		0.3002(1)
<i>x</i> = 0.4	as-prepared	0.38189(2)	1.5629(1)	0.29755(1)
	acid-exchanged	0.37763(2)	1.7921(1)	0.30069(1)
	nanosheet	0.3772(1)		0.3006(1)
<i>x</i> = 0.6	as-prepared	0.38157(1)	1.5652(1)	0.29746(1)
	acid-exchanged	0.37723(1)	1.8017(1)	0.30073(1)
	nanosheet	0.3772(1)		0.3006(1)

Table 2. Chemical analysis results of Fe,Co-doped layered titanates and acid-exchanged forms.

Fe-doping	as-prepared				after acid-exchanged			
	[K _{0.8} Ti _{(5.2-2x)/3} Li _{(0.8-x)/3} Fe _x O ₄]				K	Li	Ti	Fe
	K	Li	Ti	Fe	K	Li	Ti	Fe
x = 0	17.4 (0.77)	1.02 (0.27)	46.0 (1.74)	0 (0)	0 (0)	0 (0)	49.8 (1.74)	0 (0)
x = 0.2	17.2 (0.80)	0.73 (0.20)	40.6 (1.60)	5.8 (0.20)	0 (0)	0 (0)	44.4 (1.60)	6.4 (0.20)
x = 0.4	16.9 (0.79)	0.48 (0.13)	36.2 (1.47)	11.4 (0.40)	0 (0)	0 (0)	39.3 (1.46)	12.6 (0.40)
x = 0.6	16.2 (0.81)	0.24 (0.07)	32.7 (1.33)	17.2 (0.60)	0 (0)	0 (0)	35.1 (1.34)	18.0 (0.59)
x = 0.8	16.4 (0.80)	-	27.8 (1.20)	21.5 (0.80)	0 (0)	-	31.4 (1.23)	23.1 (0.77)
Co-doping	[K _{0.8} Ti _{(5.2-y)/3} Li _{(0.8-2y)/3} Co _y O ₄]				K	Li	Ti	Co
	K	Li	Ti	Co	K	Li	Ti	Co
y = 0.1	17.2 (0.88)	0.66 (0.19)	40.7 (1.70)	3.2 (0.11)	0 (0)	0 (0)	40.7 (1.70)	3.2 (0.11)
y = 0.2	16.2 (0.80)	0.49 (0.13)	40.0 (1.61)	5.9 (0.19)	0 (0)	0 (0)	39.8 (1.66)	5.9 (0.20)
y = 0.3	16.2 (0.80)	0.21 (0.06)	39.3 (1.58)	8.8 (0.29)	0 (0)	0 (0)	39.5 (1.65)	8.8 (0.30)
y = 0.4	16.4 (0.81)	-	38.8 (1.56)	11.2 (0.37)	0 (0)	-	38.8 (1.62)	11.2 (0.38)
Fe/Co-codoping	[K _{0.8} Ti _{1.6-x/2} Fe _x Co _{0.4-x/2} O ₄]				K	Ti	Fe	Co
	K	Ti	Fe	Co	K	Ti	Fe	Co
x = 0.1	15.5 (0.80)	30.9 (1.30)	16.6 (0.60)	3.1 (0.11)	0 (0)	33.2 (1.31)	17.2 (0.58)	3.3 (0.11)
x = 0.2	16.3 (0.85)	33.0 (1.40)	10.9 (0.40)	5.9 (0.20)	0 (0)	35.6 (1.40)	11.7 (0.39)	6.4 (0.20)
x = 0.3	16.5 (0.86)	35.4 (1.50)	5.4 (0.20)	8.9 (0.31)	0 (0)	38.3 (1.50)	5.9 (0.20)	9.6 (0.31)

wt% (atomic ratio)

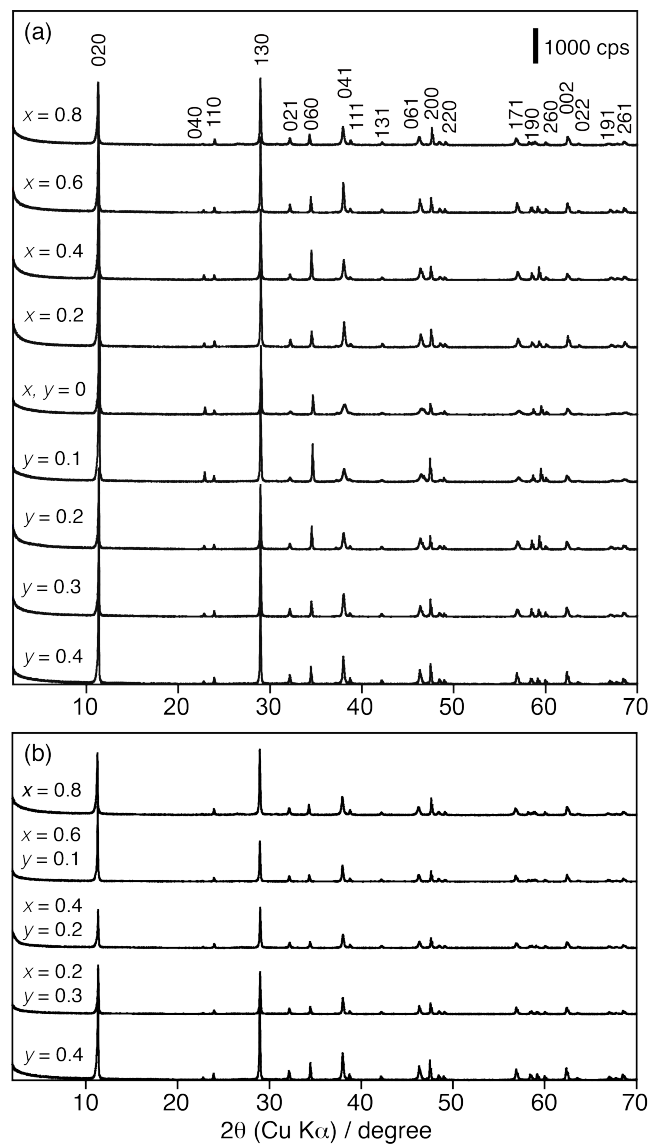


Figure S1. XRD patterns of (a) (Li/Fe)- and (Li/Co)-cosubstituted layered titanates ($\text{K}_{0.8}\text{Ti}_{(5.2-2x)/3}\text{Li}_{(0.8-x)/3}\text{Fe}_x\text{O}_4$ and $\text{K}_{0.8}\text{Ti}_{(5.2-y)/3}\text{Li}_{(0.8-2y)/3}\text{Co}_y\text{O}_4$) and (b) (Fe/Co)-codoped layered compounds ($\text{K}_{0.8}\text{Ti}_{1.6-x/2}\text{Fe}_x\text{Co}_{0.4-x/2}\text{O}_4$).

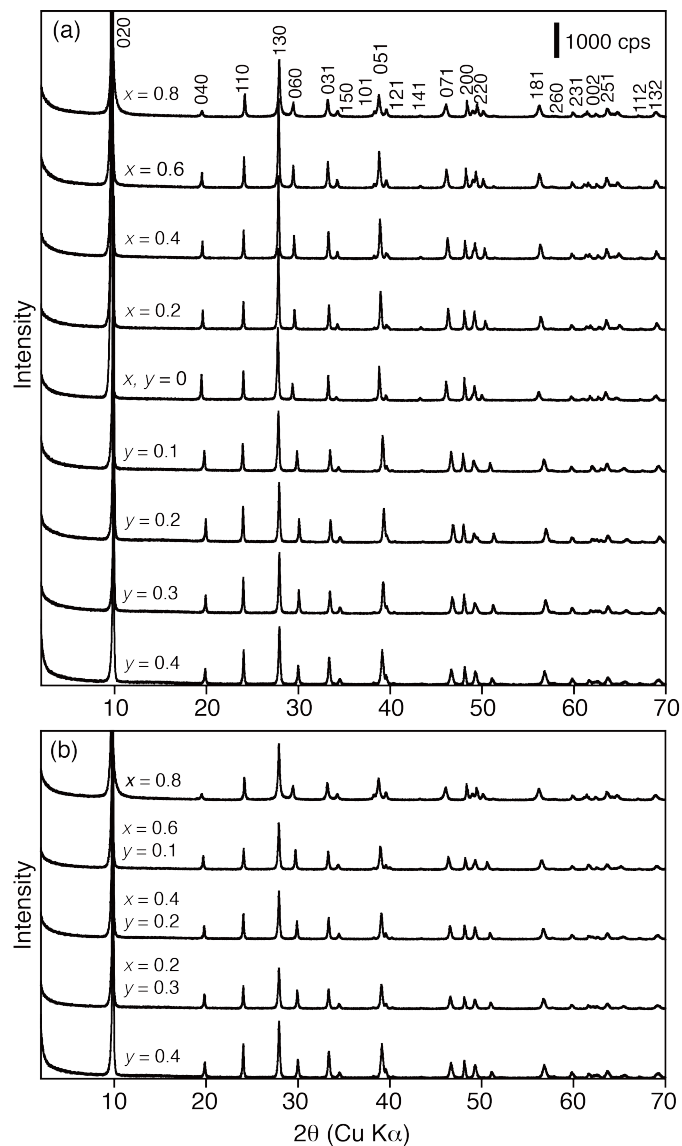


Figure S2. XRD patterns of the acid-exchanged forms. (a) $H_{(3.2-x)/3}Ti_{(6.4-2x)/3}Fe_xO_4 \cdot nH_2O$ ($x = 0.0 - 0.8$), $H_{(3.2-2y)/3}Ti_{(5.2-2y)/3}Co_yO_4 \cdot nH_2O$ ($y = 0.0 - 0.4$). (b) $H_{0.8}Ti_{1.6-x/2}Fe_xCo_{0.4-x/2}O_4 \cdot nH_2O$ ($x = 0.0 - 0.8$)

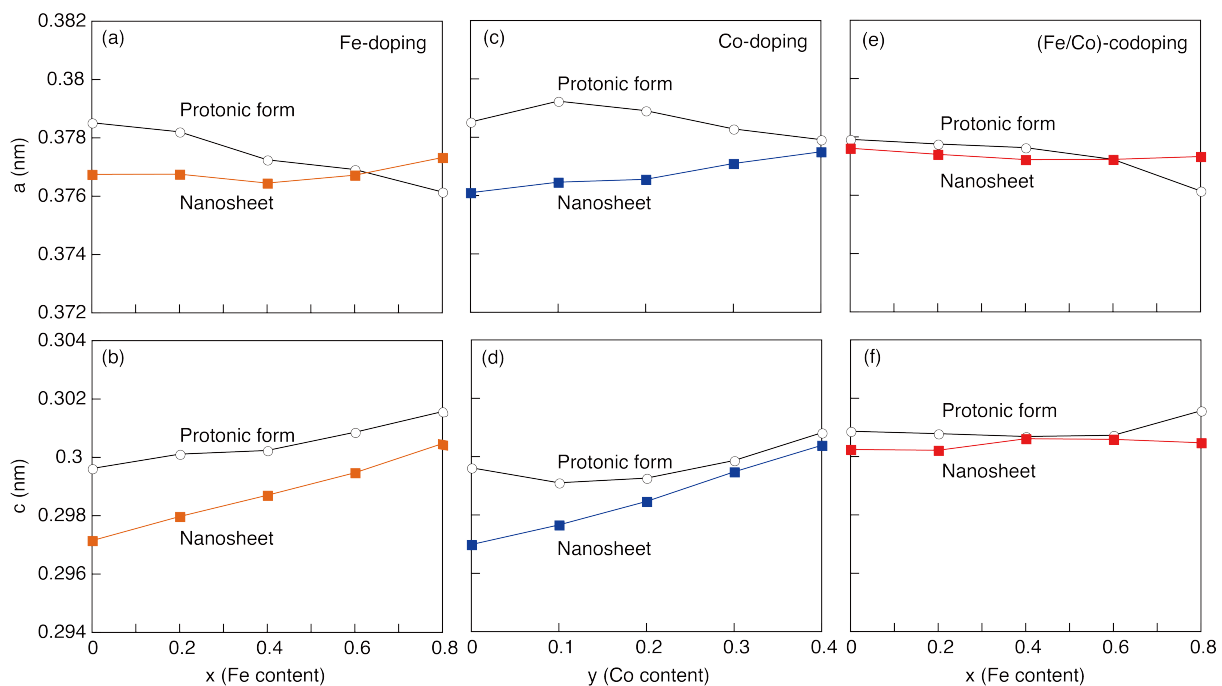


Figure S3. Variation of the in-plane lattice parameters of protonic titanates and exfoliated nanosheets. (a), (b) $\text{H}_{(3.2-x)/3}\text{Ti}_{(6.4-2x)/3}\text{Fe}_x\text{O}_4 \cdot n\text{H}_2\text{O}$ and their nanosheets ($x = 0.0 - 0.8$), (c), (d) $\text{H}_{(3.2-2y)/3}\text{Ti}_{(5.2-2y)/3}\text{Co}_y\text{O}_4 \cdot n\text{H}_2\text{O}$ ($y = 0.0 - 0.4$) and their nanosheets, (e), (f) $\text{H}_{0.8}\text{Ti}_{1.6-x/2}\text{Fe}_x\text{Co}_{0.4-x/2}\text{O}_4 \cdot n\text{H}_2\text{O}$ ($x = 0.0 - 0.8$) and their nanosheets. In each case, the standard deviation is within the symbol.

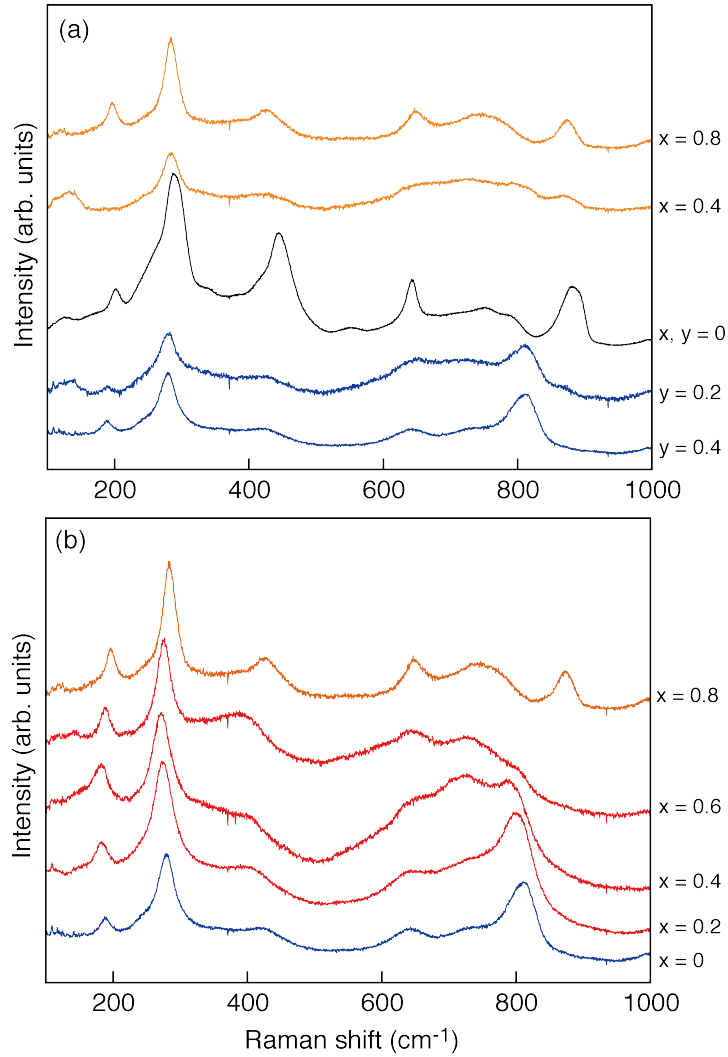


Figure S4. Raman spectra of (a) $\text{K}_{0.8}\text{Ti}_{(5.2-2x)/3}\text{Li}_{(0.8-x)/3}\text{Fe}_x\text{O}_4$, $\text{K}_{0.8}\text{Ti}_{(5.2-y)/3}\text{Li}_{(0.8-2y)/3}\text{Co}_y\text{O}_4$ and (b) $\text{K}_{0.8}\text{Ti}_{1.6-x/2}\text{Fe}_x\text{Co}_{0.4-x/2}\text{O}_4$. Local structural features induced by (Li /Fe) and (Li/Co) cosubstitution are noticeable in the high-frequency region ($600 - 900 \text{ cm}^{-1}$). The most notable changes are the softening and reduced intensity of 650- and 900-cm^{-1} modes. These Raman modes stem from Ti-O bonds in TiO_6 octahedral host layers,^[17] and thus spectral modification in this region are strongly correlated to the nature of the lattice dopants in the octahedral Ti sites. These results indicate that the Fe, Co ions were fully incorporated into Ti sites in the host layers. Raman spectra in $\text{K}_{0.8}\text{Ti}_{1.6-x/2}\text{Fe}_x\text{Co}_{0.4-x/2}\text{O}_4$ also showed structural changes in TiO_6 octahedral host layers upon Fe/Co doping, supporting the structural model on (Fe/Co) co-substitution into Ti sites.

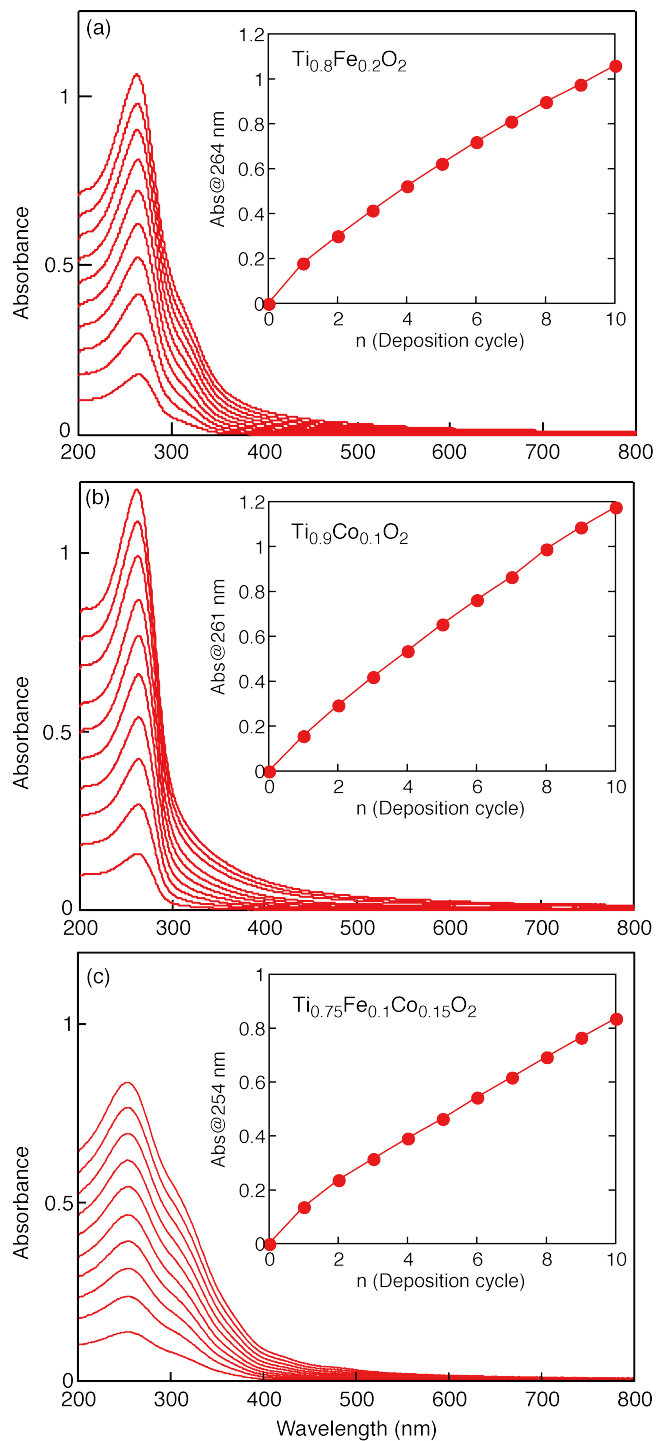


Figure S5. UV-Visible absorption spectra for multilayer films of (a) $[\text{PDDA}/\text{Ti}_{0.8}\text{Fe}_{0.2}\text{O}_2]_n$, (b) $[\text{PDDA}/\text{Ti}_{0.9}\text{Co}_{0.1}\text{O}_2]_n$ and (c) $[\text{PDDA}/\text{Ti}_{0.75}\text{Fe}_{0.1}\text{Co}_{0.15}\text{O}_2]_n$ ($n = 0 - 10$) assembled on a quartz glass substrate. (Inset) The observed absorbance at the peak top position as a function of the deposition cycle. The absorption band around 260 nm is characteristic of titania nanosheets, and its nearly linear increment as a function of the number of deposition cycles indicates a stepwise and regular film growth.

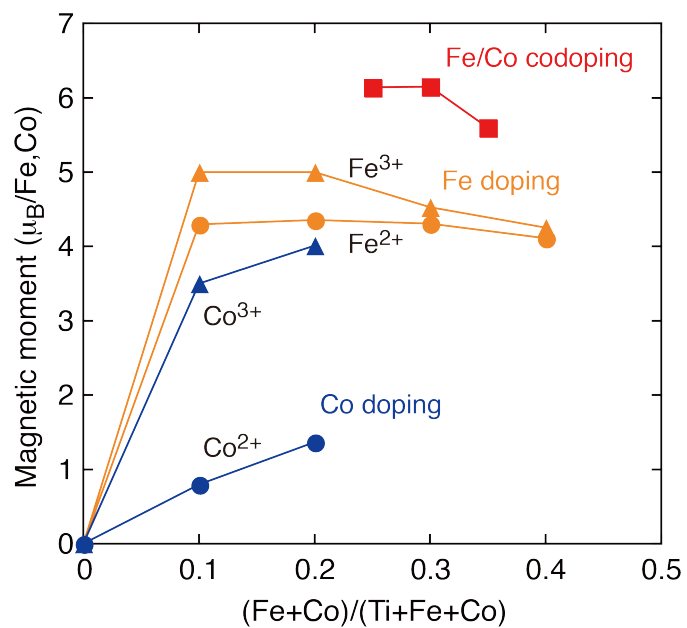


Figure S6. First-principles DFT calculations on the magnetic properties of $\text{Ti}_{1-x}\text{Fe}_x\text{O}_2$, $\text{Ti}_{1-y}\text{Co}_y\text{O}_2$ and $\text{Ti}_{1-x-y}\text{Fe}_x\text{Co}_y\text{O}_2$ nanosheets with different oxidation states.

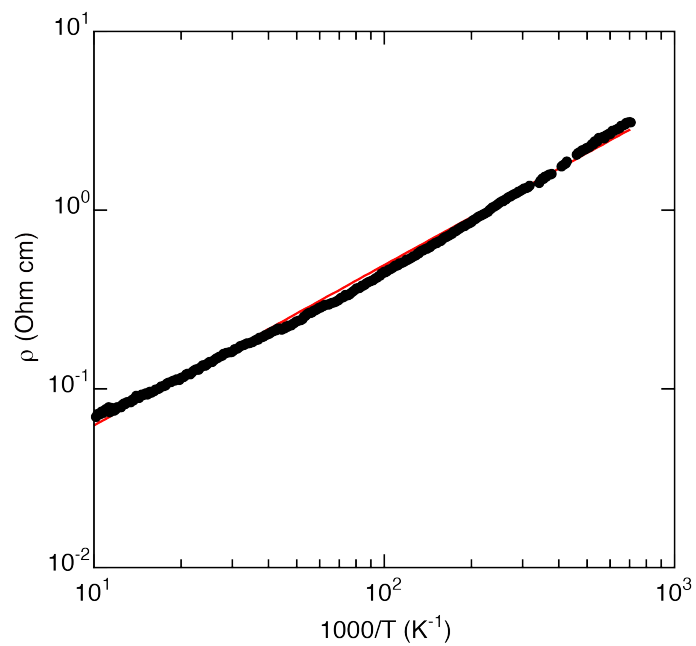


Figure S7. Resistivity versus the reciprocal temperature of $\text{Ti}_{0.75}\text{Fe}_{0.1}\text{Co}_{0.15}\text{O}_2$ nanosheets, calculated from Figure 10a. The measured resistivity was fitted as a function of $1/T$ according to the Arrhenius-type expression $R = R_0 \exp(-E_a/kT)$, where R is the electrical conductivity, R_0 is the pre-exponential factor, k is the Boltzmann constant, and E_a is the activation energy.